Medicine in Novel Technology and Devices 20 (2023) 100271

Contents lists available at ScienceDirect

Medicine in Novel Technology and Devices

journal homepage: www.journals.elsevier.com/medicine-in-novel-technology-and-devices/

Effect of the antenna slot numbers and position on the performance of microwave ablation

Sabiha Binte Aziz [a,b], Md Rejvi Kaysir [b,c,*], Md Jahirul Islam [b,**], Torikul Islam [a,b,d], Mahmudur Rahman [e]

[a] Department of Biomedical Engineering (BME), Khulna University of Engineering & Technology, Khulna-9230, Bangladesh
[b] Photonics Research Group, Department of EEE, Khulna University of Engineering & Technology, Khulna-9230, Bangladesh
[c] Department of Electrical and Computer Engineering, Waterloo Institute for Nanotechnology, University of Waterloo, 200 University Ave, Waterloo, ON, Canada
[d] Department of Biomedical Engineering (BME), New Jersey Institute of Technology, Newark, NJ, USA
[e] Department of Electrical and Electronic Engineering, Dhaka University of Engineering & Technology, Gazipur 1707, Bangladesh

ARTICLE INFO

Keywords:
Microwave ablation (MWA)
Finite element method (FEM)
Liver tumor
Microwave antenna
Specific absorption rate (SAR)

ABSTRACT

Microwave ablation (MWA) is a type of thermal ablation used for cancer treatment in interventional radiology. To induce localized tissue heating MWA employs electromagnetic waves within the microwave energy spectrum, which is done by the precisely designed antenna. This study substantially emphasizes the design and performance ameliorating of slot (both single and double) antennae and compares the results with conventional monopole antennae in terms of temperature distribution, specific absorption ratio (SAR), and thermal tissue damage rate. The simulation has been done in COMSOL by solving the Bioheat equation along with Maxwell electromagnetic equations using the finite element method. The simulation results reveal that the double-slot antenna has the most accurate and directional heat dissipation for liver tumors as well as the highest tissue damage rate and SAR. The highest SAR was found to be 3500 W/kg and 3350 W/kg at the implant depth of 61 mm and 63 mm for double and single-slot antennae, respectively. In addition, the fastest tissue damage occurred near the upper slot of the double-slot antenna. This study helps to understand the basic design parameters for enhancing single and double-slot antennae performance.

1. Introduction

Hyperthermia is a tumor therapy approach in which energy is delivered to the cells in human tissue to elevate their temperature to damage or ultimately kill tumor cells while intending to not harm the healthy cells [1]. Thermal therapy, also known as thermal ablation, is a local cancer treatment approach that involves providing external heat energy to the tumor owing to elevate the temperature over 50–60 °C [1,2]. Chemotherapy and radiation therapy, for example, are conventional treatments that do not always produce the desired results as well as it has serious side effects on the patient's body due to the toxicity of anti-cancer agents [3]. Thus, noninvasive or minimally invasive thermal therapy is an alternative approach for treating tumor cells. Ablation is a process of selectively killing a precise target tissue by applying heat-based radio-frequency (RF) ablation and microwave ablation, cold-based (cryo-therapy), chemical-based (percutaneous ethanol injection), or direct applying laser hyperthermia to a tumor, resulting in rapid cell death [4]. Cryosurgery uses special cryoprobes for directional cell damage but there is the use of cryo-fluid flowing through the interior of the antenna and freezing the cancer cell. It has complexity in practical usages as well as uncertainty to damage the healthy cell. On the contrary, chemical treatment has complexity with adequate chemical injection through an artery. RF ablation has recently been used for liver cancer, but heat sink and higher impedance of ablated tissue are significant limitations [5]. Microwave Ablation (MWA) is a relatively innovative discovery in the realm of thermal treatment due to its non-severe damage to internal organs and comparatively fewer side effects [5]. A remarkable feature of MWA is that it elevates the temperature over the threshold level of normal physiology to eradicate cancer cells like primary and secondary liver cancer, as well as kidney, lung, and bone cancers [6,7]. It should be noted that MWA yields better results than other non-invasive techniques found in the concurrent literature [8]. However, there are some

* Corresponding author. Photonics Research Group, Department of EEE, Khulna University of Engineering & Technology, Khulna-9230, Bangladesh.
** Corresponding author.
E-mail addresses: rejvi@eee.kuet.ac.bd (M.R. Kaysir), jahirul@eee.kuet.ac.bd (M. Jahirul Islam).

https://doi.org/10.1016/j.mednotd.2023.100271
Received 30 April 2023; Received in revised form 14 October 2023; Accepted 19 October 2023

drawbacks to using MWA such as the antenna exhibits drawback current and backward heating due to the shape of the antenna. To alleviate this issue, different antenna design and their placement in tumor sites were investigated by different research groups [9–12]. A group of researchers reported the use of a deformation correction factor to a therapeutically applicable rigid registration methodology within the implementation of image-guided MWA to demonstrate enhanced localization and antenna placement in a deformable hepatic phantom for the improvement of this strategy [13].

As stated, the prime goal of thermal ablation is to elevate the tissue temperature and stimulate acute coagulative necrosis without damaging surrounding healthy tissue. The most common antennas used in MWA are slot coaxial antennas because of their low cost and compact dimension, thus coaxial-based antennas are critical for MWA applications [8]. Previously, different types of antennae such as monopole [13,14], dipole, helical [9], triaxial [10], choked [11,15], sleeved [15], and slot antennas have been designed in this field. In a recently published report, a ring-shaped slot antenna was designed [16] with an inner and outer conductor focusing on the Self Absorption Ratio (SAR) for analyzing the fraction of tissue damage. Other studies demonstrated the possibility of a micro-coaxial double slot antenna to create MWA for the treatment of bone cancer and liver tumors [17,18]. Some research findings focused on designing new types of coaxial antennae owing to increased efficiency in treating cancer cells [18,19]. As the shape, size, and placement of the tumor in the human body vary, it cannot be treated with a particular design of antenna efficiently. Thus, a lot of factors (both internal and external) need to be considered when designing an antenna for different locations of the body. As different parameters change the outcomes for tissue damage in MWA, different system parameters were analyzed in the literature based on disparate input frequencies, microwave power absorbed, temperature distribution, and SAR distribution [12,17]. In addition, some studies focused on different antenna parameters for treating cancer cells by varying tumor size, shape, and depth at different locations of the human body.

In general, a coaxial wire in an interstitial antenna in an MWA probe transmits electromagnetic (EM) energy into the desired tissue around the antenna. The tiny diameter of this probe is a significant requirement for a minimally invasive ablation process [20]. As a result, the conventional design is limited to coaxial applicators, where power absorption elevates the temperature of the local tissue, resulting in cell damage. MWA is a minimally invasive alternative to surgical tumor excision, with shorter recovery periods and a viable treatment choice for cancer patients who cannot undergo surgery. Most of the study in the literature uses Microwave frequencies of 915 MHz and 2.45 GHz due to the production of lethal temperature from the applied EM field for tissue destruction [6,17, 21,22]. Coaxial antennas are generally inserted into the desired area of the tissue and then the oscillating EM field in the tissue causes water molecules to vibrate, resulting in frictional heating. When the temperature rises more than 52 °C, the corresponding tumor cell starts to damage [8]. The clinical treatment with a microwave antenna must be concerned with the fact of surrounding healthy tissue damage as the EM wave radially propagates to the surrounding area of the tumor and also controls the lesion generation accurately [17,19]. As a lot of parameters are involved in MWA, heat transfer modeling is required to comprehend the real mechanism of MWA inside human tissue to damage the cancer cell effectively without affecting the surrounding healthy tissues. Most importantly, as the antenna parameters are crucial in the MWA process, it is imperative to investigate the antenna parameters' effects on the performance of conventional MWA.

In this study, we primarily designed and investigated the output performance of coaxial antennas (both single and double slots) by varying the design parameters and comparing them with monopole antennae to demonstrate the performance of MWA for human Liver tissues. The output performance is compared based on the SAR rate, specific tissue damage rate, and temperature distribution. In addition, the temperature and EM power dissipation for different slot numbers of coaxial antennas are analyzed here. The numerical simulation was performed using COMSOL Multiphysics software, where antennas were designed in 2D asymmetric view owing to less computational analysis. Finite Element Method (FEM), which refers as widely utilized in cardiac and hepatic RFA simulations, is ideally adapted to heat transfer issues because it can give users a rapid and precise solution to various systems of differential equations [16,19]. The degree of damage is proportional to the temperature attained as well as the treatment period. Because only the highest temperature cannot describe the ablation zone precisely, mathematical models for cell response to temperature rise were also considered in this study, which was based on the Arrhenius model [2]. Also, a 2.45 GHz microwave frequency was used in this work as it can produce a larger ablation zone because more power is accumulated close to the antenna slots and thermal conduction plays a larger role [22].

2. Microwave ablation model and simulation procedure

2.1. Geometry and problem statement

This study compares single and double-slot coaxial microwave antennae for liver tumor hyperthermia treatment and compares them with conventionally used monopole antennae. Fig. 1 shows the model features and geometries of the antennae considered in this work. The material and properties of these antennae are selected from the previously published literature [8,13,23]. It comprises a narrow coaxial cable with a 1 mm ring-shaped slit cut away from the short-circuited tip of the outer conductor as shown in Fig. 1 because the electric field intensifies close to the slot, the interstitial heating depends greatly on the effective heating around the antenna's tip. Slots were made for discharging microwave radiation, and the tip end was soldered in an appropriate place. Three alternative geometries of antennas (monopole, single slot, and double slot) were built from coaxial cables for this study.

The antenna has an outer and inner conductor and is inserted about 70 mm deep into the liver tissue. The dielectric layer is 1.68 mm in diameter and is surrounded by catheter coating. The catheter is made of polytetrafluoroethylene (PTFE) to maintain hygiene and proper electromagnetic waveguide purpose [23]. The diameter for the outer and inner conductors are 1.19 mm and 0.94 mm, respectively, because a thin antenna is required for interstitial treatment [3,8,19,21]. In this heat-producing antenna, the dielectric material is considered liver tissue, and its permittivity and electric conductivity are used in the model. It is noted that heat absorption by the tissue depends on the function of its dielectric permittivity and conductivity. The summary of the geometrical design parameters is shown in Table 1.

This ablation system operates at 2.45 GHz microwave frequency as it can produce a larger ablation zone [3,20,24]. For the monopole antenna, there is a radiating segment 14 mm long [14]. For slot antenna, the effective wavelength at 2.45 GHz is utilized to determine the slot spacing [8,20,24,25]. The equation for effective wavelength (λ_{eff}) is calculated by the following equation,

$$\lambda_{eff} = \frac{v}{f\sqrt{\varepsilon_r'}} \tag{1}$$

Here, v represents the speed of light, and f is the operating frequency of the microwave generator which is 2.45 GHz. ε_r' represents the relative permittivity of the liver tissue which is 42.50 [14,17,24]. The value for λ_{eff} is found to be 18.8 mm from Equation (1).

According to a preliminary study, the best antenna design should be achieved by considering slot widths between 1 and 10 mm [7,17]. In this study, each slot's height and diameter were considered to be 1 mm and 0.85 mm, respectively. First, the slot was located at $\lambda_{eff}/8 = 2.35$ mm from the antenna tip and the second slot was located at $\lambda_{eff}/4 = 4.7$ mm from the first slot. One of the main reasons for choosing slot distance precisely was due to the temperature distribution rate and power deposition localization that occur in the distal tip of the antenna. Fig. 1 shows

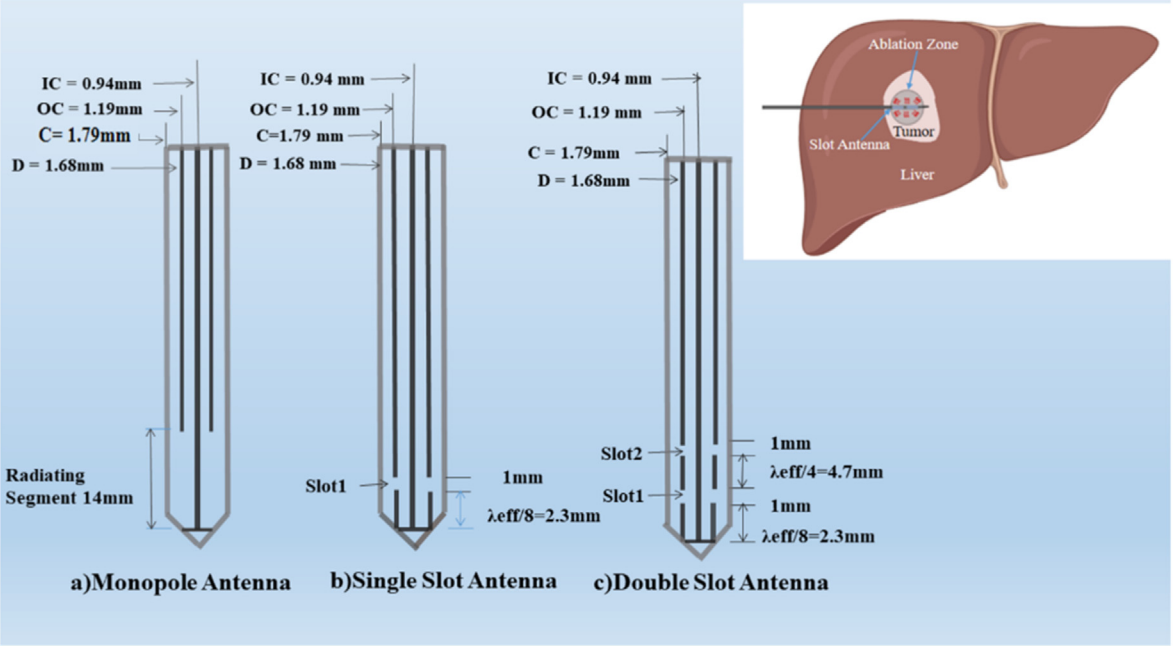

Fig. 1. Schematic representation of the geometry model of the (a) monopole, (b) single slot, and (c) double slot antenna. Here, IC: Inner Conductor, OC: Outer Conductor, C: Catheter, D: Dielectric. [Inset: Overview of the MWA process for liver tissue].

Table 1
The geometrical properties of Microwave Antenna for both monopole and slot (single and double) antennas.

Material	Diameter (mm)	Height (mm)
Outer conductor	1.19	70
Inner conductor	0.94	69.9
Dielectric	1.68	69.9
Catheter	1.79	70
Central conductor	0.29	69.9
Slot	0.85	1
Radiating Segment	1.68	14

the geometry of single and double-slot antennas with the considered design parameters.

This model calculates the temperature distribution, damage rate, and SAR in liver tissue, which is defined as the ratio of absorbed heat power to tissue density. It uses rotation symmetry problems, which allows us to use 2D cylindrical geometry instead of a 3D problem. This 2D geometry helps to solve complex problems in a computationally convenient way. The overall MWA process with the antenna insertion mechanism to the liver tissue is shown in the inset of Fig. 1.

2.2. Computational procedures

2.2.1. Numerical method

The numerical analysis was done using Finite Element Method (FEM) in COMSOL Multiphysics Software. This type of model is ideally suited to heat transport issues like ablation because it can offer users rapid, precise solutions to various systems of differential equations [8]. The proposed numerical analysis is based on several mathematical models that will be discussed in the next subsections. The designed coaxial slot antenna shows rational symmetry around the longitudinal axis, therefore, using a 2D asymmetric model minimizes the complexity and computational time. This FEM model assumes the surrounding liver tissue is homogeneous [23]. The axisymmetric finite element mesh was chosen to strike a balance between model dimensionality and computing accuracy [20,23]. The user-controlled mesh was used in this model where a maximum element size of 3 mm and minimum size of 0.024 mm was defined depending on the different regions of the geometry. Free triangular shape of elements have been chosen due to the Lagrange quadratic shape function [20]. Comparatively finer mesh zone is created near the tip of the antenna and the slot of the antenna where the temperature is highest. The electromagnetic waveguide analysis and Bioheat equation were used for thermal distribution to biological tissue. In the electromagnetic wave analysis, a scattering boundary condition is applied to that surface. This condition ensures that the boundary doesn't interfere with the distribution of the electromagnetic field. In addition, the model considers the wall of MWA as a perfect electric conductor, and the dielectric property of liver tissue is determined as a function of temperature. Moreover, the adiabatic boundary condition is applied in between the outer surface of antenna and hepatic tissue. Initial and related boundary condition based partial differential equations are coupled and iterated at each triangular mesh in one time step. Within the liver tissue, there is no energy exchange via outer surface and no chemical reaction occurs. The thermal damage was calculated conveniently by using the Arrhenius equation [11,14,23].

2.2.2. Electromagnetic wave propagation

A three-dimensional FEM was used for solving EM field and temperature distribution. The EM energy propagation was determined by the dielectric permittivity and magnetic permeability of the propagation medium [3]. The model considers a coaxial antenna's wall to be a perfect electric conductor (PEC) [6]. The medium between the antenna and the tissue was considered to be homogeneous, linear, and isotropic. A transverse electromagnetic (TEM) field characterizes an electromagnetic wave traveling in a coaxial wire. The waveguide imposes boundary constraints on the wave, resulting in transverse electromagnetic modes (TEM), which are calculated from Maxwell's equations. This model of the electric and magnetic field with TEM based on time variation is expressed in 2D asymmetric cylindrical coordinates [17,26].

$$E = e_r \pi \frac{C}{r} e^{j(\omega t - kz)} \tag{2}$$

$$H = e_\varphi \frac{C}{rZ} e^{j(\omega t - kz)} \tag{3}$$

Here, $C = \sqrt{\frac{ZP}{\pi \ln r_o/r_i}}$, E is the electric field, and H is the magnetic field perpendicular to each other. Z defines the wave impedance for the dielectric property of the antenna and ω is the angular frequency. From Equations (2) and (3) the time average power flow for the coaxial antenna was derived from Maxwell's Electromagnetic field condition [15,17].

$$\boldsymbol{P}_{av} = \int_{r_i}^{r_o} R_e\left(\frac{1}{2}E \times H\right) 2\pi dr = e_z \pi \frac{c^2}{z} ln\frac{r_o}{r_i} \tag{4}$$

Here, r_o indicates the radius of the outer conductor and r_i indicates the radius of the inner conductor. P_{av} is the average power flow through the antenna, (r, z, φ) are the components of cylindrical coordinates. The magnetic field in liver tissue changes only in the azimuth direction. As a result, axis-symmetric transverse magnetic (TM) wave formulation characterizes the antenna. Here H_φ is azimuth direction magnetic component simplified as,

$$\nabla \times \left(\left(\varepsilon_r - \frac{j\sigma}{\omega\varepsilon_o}\right)^{-1} \nabla \times \overrightarrow{H_\varphi}\right) - \mu_r K^2 \overrightarrow{H_\varphi} = 0 \tag{5}$$

Here, $\varepsilon_o = 8.854 \times 10^{-12}$ F/m denotes the permittivity of free space, ω is the angular frequency, K is the propagation constant defined as $K = \frac{2\pi}{\gamma}$. ε_r (μ_r) is the medium relative permittivity (permeability).

Thermal and electromagnetic properties which are the input parameters for the liver, dielectric, and blood are shown in Table 2 [3,8,17]. These values were considered as the initial values when solving the differential equation in COMSOL environment. In this model, antennas were considered to be a PEC to assume rigid body motion between antenna surface and liver tissue for simplicity and avoiding numerical error due to body motion and internal resistance, hence the following metallic surface boundary condition was considered.

$$n \times E = 0 \tag{6}$$

The first order scattering boundary condition was applied to the remaining surface of the model with an input field $H_{\varphi 0}$. The scattering boundary condition was selected for the outside surface of liver tissue to prevent reflection artifacts.

$$n \times \sqrt{\varepsilon}\overrightarrow{E} - \sqrt{\mu}\ \overrightarrow{H_\varphi} = -2\sqrt{\mu}\ \overrightarrow{H_{\varphi 0}} \tag{7}$$

Here, $\overrightarrow{H_{\varphi 0}} = \frac{C}{Z_r}$ and $H_{\varphi 0}$ is the excitation magnetic field. Antenna spherical wave generation was calculated as follows,

$$n \times \left(\nabla \times \overrightarrow{H_\varphi}\right) - jK\overrightarrow{H_\varphi} = 0 \tag{8}$$

The location of microwave energy deposition within liver tissue was predicted using the changes in tissue's dielectric properties. The change in tissue permittivity due to heat when the temperature of liver tissue was elevated, increased from 37 °C to over 100 °C was around 5 %. The corresponding boundary conditions are shown in Fig. 2.

Table 2
Thermal and electromagnetic properties of dielectric, Liver tissue, and slot antenna.

Electromagnetic properties	Value (unit)	Thermal properties	Value (unit)
Electric conductivity (Liver)	1.69 s/m	Heat Capacity (liver)	3600 J/(kg.K)
Relative permittivity (Liver)	43.03	Thermal Conductivity (liver)	0.52 W/(m·K)
Electric conductivity (dielectric)	0	Specific heat (blood)	3639 J/(kg·K)
Relative permittivity (dielectric)	2.1	Blood temperature	310.15 K
Relative permittivity (Catheter)	2.60	Density (liver)	1060 [kg/m^3]
Electric conductivity (Slot)	0	Blood perfusion rate	0.0036 1/s

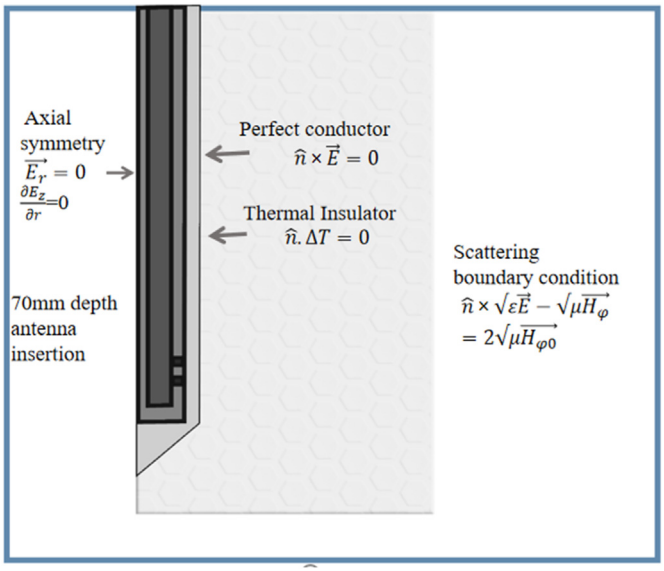

Fig. 2. Representation of the boundary condition, thermal insulator, and perfect electric conductor condition for a 2D asymmetric view of MWA.

2.2.3. Heat transfer analysis through MWA

The thermal distribution through biological tissue can be calculated using Penne's Bioheat Equations. The radial thermal propagation was calculated through Heat Transfer analysis for MWA.

$$\rho c \frac{\partial T(r,t)}{\partial t} = \nabla(k\nabla T(r,t)) + \rho_b C_b \omega_b (T_b - T) + Q_{ext} + Q_m \tag{9}$$

Where k is the liver's thermal conductivity (W/(m·K)), b represents the blood density (kg/m^3), c is the blood's specific heat capacity (J/(kg·K)), ω_b denotes the blood perfusion rate (1/s), and T_b is the arterial blood temperature (K). Additionally, Q_{ext} is the heat source from metabolism, and Q_{ext} is an external heat source, both are measured in W/m^3 and the left side of the equation defines the transient term. ρ_b is found to be 33,800/m^3 for liver tissue [12,17,27] and depends on the electric conductivity property of liver tissue.

Moreover, the heat transfer was considered to have happened solely in the tissue domain, with a starting temperature of 37 °C. In all domains, the starting temperature was $T_b = 37$ °C. The model assumes that the blood perfusion rate is $\omega_b = 0.0036$ s^{-1} and the specific heat capacity of blood is $C_b = 3639$ J/(kg.K). Where the temperature-dependent blood perfusion rate was defined as [14,17]

$$\omega_b(T) = 0.000021T + 0.0036 \tag{10}$$

Furthermore, Only the liver tissue domain was considered in the heat transfer study. The liver tissue's borders were regarded as insulating boundary conditions:

$$n.(K\nabla T) = 0 \tag{11}$$

2.2.4. Specific absorption rate (SAR)

In dosimetry experiments, the SAR is a fundamental variable that was computed and analyzed. The SAR is the amount of non-ionizing radiation power (or rate of absorbed energy) absorbed per mass of biological tissue in watts per kilogram (W/kg) [17]. When microwave radiation is absorbed by liver tissue and converted to internal heat production, the tissue temperature escalates. SAR is directly determined from the Pennes Bioheat equation [3,17]. As Q_{ext} is dependent on the liver conductivity (σ_{liver}) and the resistive heat. Q_{ext} is created by the electromagnetic field

which is equivalent to the external heat source:

$$Q_{ext} = \frac{1}{2}\sigma_{liver}\vec{E}^2 \tag{12}$$

The electrical properties are massively dependent on the change of temperature and the SAR measures the amount of electromagnetic power deposited in tissue.

$$SAR = \frac{\sigma_{liver}}{2\rho_{liver}}\vec{E} \tag{13}$$

$$Q_{ext} = \rho_{liver} \times SAR \tag{14}$$

Now, the heat dissipation can be represented by the following Equation (15), where all the parameters are described earlier.

$$\rho c\frac{\partial T(r,t)}{\partial t} = \nabla(k\nabla T(r,t)) + \rho_b C_b \omega_b (T_b - T) + Q_m + (\rho_{liver} \times SAR) \tag{15}$$

2.2.5. Thermal injury

The Arrhenius equation can be used to directly measure thermal damage and cell necrosis. The Arrhenius fit parameters indicate the likelihood of cell damage for a given exposure temperature and duration. At high temperatures, Arrhenius parameters have been determined in various bodily tissues, including the liver [[3,28]].

$$\Omega(t) = ln\frac{c(0)}{c(t)} = \int_0^t A.e^{-\frac{\nabla E}{RT}}dt \tag{16}$$

Where $\Omega(t)$ is thermal damage rate constant, A is the pre-exponential factor, ∇E is the activation energy, R is the universal Gas constant, and T is temperature.

3. Results and discussion

This section elaborately delineates the simulation procedure and results in comparison among monopole, single, and dual slot antennae for temperature variation, SAR, tumor tissue damage rate, and ablation region depending on time variation. FEM was used to examine the transient issue and localized heat generation was scrutinized by performing electromagnetic calculations of liver tissue different parameters. The microwave power source was placed at the upper end of the antenna and primarily considered as 10 W. In this study, the EM energy and temperature distribution are solved by using an implicit time-step approach. A total of 10 min of microwave heating was considered with a time step of 15 s used to solve the bioheat equation and EM wave propagation.

To determine the validity of all the parameters and mathematical model of the designed antenna the simulation results are compared with the earlier research by Yang et al. [29]. In this process, 75 W microwave power is applied for 150s at 2.45 GHz frequency to observe the thermal distribution of liver tissue. Our designed antenna shows good agreement with the previous model with 3.14 % and 6.1 % of variation due to the difference thermal properties of catheter and dielectric.

There are some previously published works based on antenna performance. P. Keangin et al. [8] investigated on heat transfer in liver tissue for single and double slot antenna. The finding was the highest SAR value 2.7 kW/kg for 300s heating time. In our design, we found highest SAR 3.1 kW/kg for 300s heating time.

3.1. Temperature distribution to liver tissue

The EM wave was converted into heat energy and dissipated to the liver tissue. In the MWA process, the heating of the liver tissue is called dielectric heating. According to the simulation results, in every antenna case, the microwave power distribution was nearly ellipsoidal around the slot, and it shows the highest values within the radiating region and decreases with the distance. That is why air and dielectric materials were used for designing slots of the antenna. The final temperature value after 10 min of starting the ablation process has been calculated for three designed antennae for different points horizontally 5 mm distant from each other and 17 mm height which are clearly shown in Fig. 3. It was shown that for double slot antenna temperature within 5 mm of depth at point (5,20) of the tissue is found to be 350 K, decreased rapidly to 310 K for 20 mm depth at point (20,20). Thus, the temperature was decreased by 6.67 % with time for the double slot antenna.

In the case of single slot antenna temperature for a 5 mm depth at point (5,20) was 344 K and it gradually decreased to 311 K for a 20 mm depth at point (20,20). This antenna shows a 5.5 % temperature reduction with time. So double slot antenna temperature decreases rapidly with the depth of tissue. The energy dissipation started from the tip of the antenna and near the slot area of the antenna. Where conventionally used monopole antenna energy dissipated radially from the radiating segment and increased up to 338 K at 5 mm depth at (5,20) point near radiating segment.

Fig. 4 shows the ablation distribution pattern of the ablated ex-vivo liver using different antennas, and the double slot antenna produces the largest ablation region and thermal dissipation than other antennae. Thermal distribution and ablation diameter are time-dependent, and it is necessary to maintain the required time for specific applications. It is depicted in the figure that after 10 min monopole antenna temperature rises to 75 °C near the radiating segment and creates an ablation region of 2 cm diameter near the antenna. On the other hand, single and double-slot antennae have a higher temperature than monopole antennae. The highest temperature found in the double-slot antenna near the upper slot is 110 °C. Here, the temperature increase rate is 11.67 % which is 5 % more than the temperature increase by the monopole antenna. On the other hand, for a single-slot antenna, the temperature value is found to be 90 °C. The rate of temperature increase here is 8.33 %. Producing heat starts dissipating from near the tip and slot.

For the double-slot antenna, the temperature distribution was organized and maintained in such a way that the highest temperature is maintained near the slot and antenna tip. Furthermore, as time passes, the temperature distribution widens. Because microwave power absorbed by the liver tissue attenuates due to energy absorption, the absorbed energy is then transformed into thermal energy, raising the liver temperature. This temperature dissipation directly depends on the liver tissue heat capacity and antenna dielectric property which is depicted in Table 3.

3.2. Power dissipation and damage rate

The fraction of tissue damage rate was calculated using the Arrhenius equation (see Table 4). It exhibits a fraction of necrosis of tumor damage. The microwave power dissipates from the dielectric as the antenna wall was considered a perfect electric conductor. And it was observed that the fastest damage occurred near the antenna and decreased rapidly with the depth of the tissue for each of the cases (Fig. 5).

It was observed from Fig. 4 that the fastest tissue damage occurred near the upper slot of the double-slot antenna, and it was 0.8. For the single-slot antenna, the damage occurred from the slot position as well but with more scattered damage than the double-slot antenna. In the monopole antenna, the lesion occurred from the radiating segment, and the fraction of damage was 0.5. It is noted that the fraction of damage value 1 represents the tumor cell death fully. According to this definition, the simulated fraction damage reaches to 1 for double slot antenna faster. It takes 0.85 min to reach fraction damage 1 near the upper slot, which is significantly faster than the other two antennae. This value represents heat lesion by absorbing energy that is strong near the slot of the antenna, which leads to high temperatures.

3.3. Specific absorption rate (SAR)

The SAR value was compared for designed antennas at the depth of

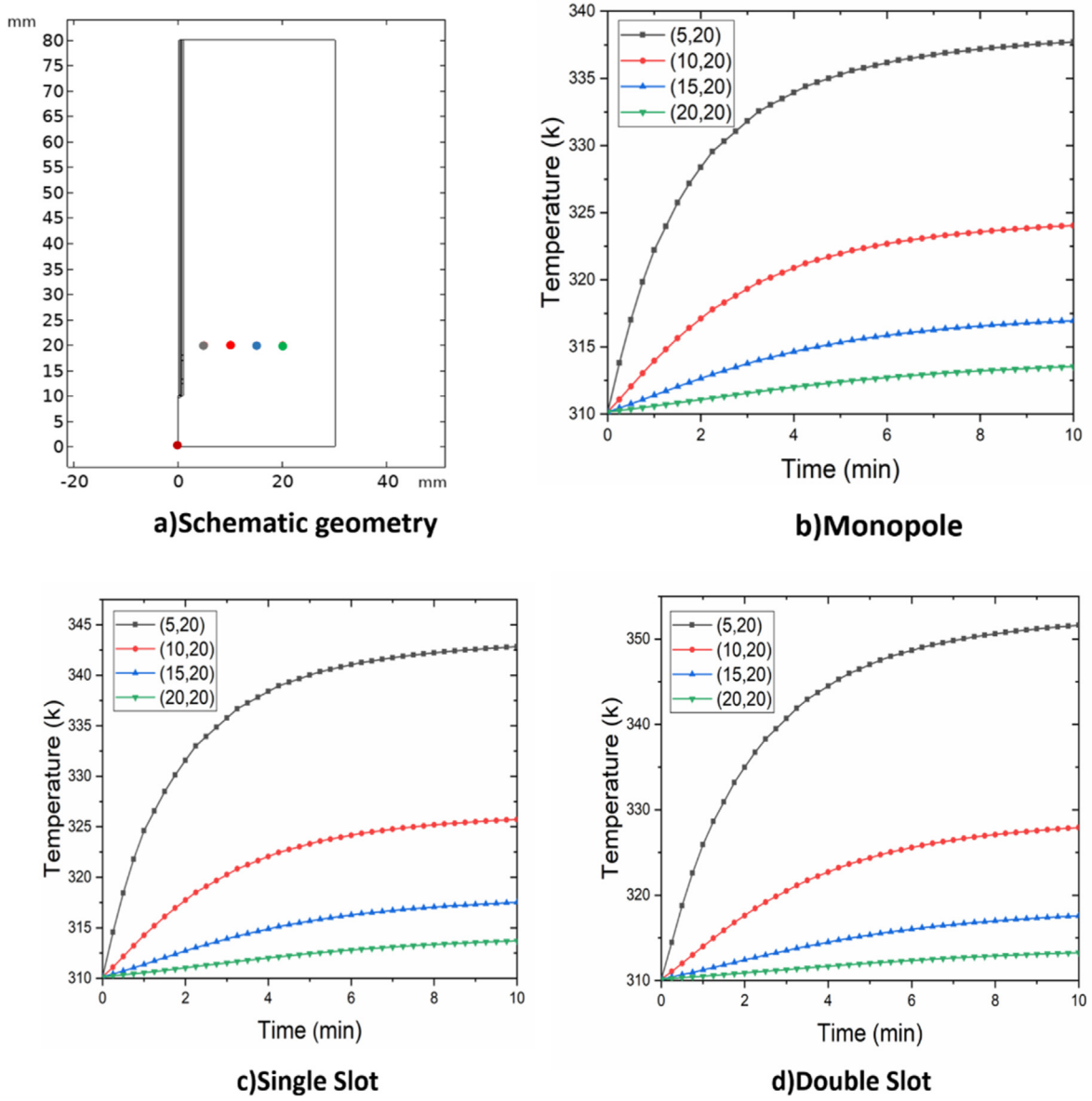

Fig. 3. (a) Schematic geometry showing four points, (b) the time evolution of the temperature of the proposed model at points (5,20), (10,20), (15,20), and (20,20) for monopole, (c) single slot, and (d) double slot antenna for 10 min of ablation start.

2.5 mm parallel line to the antenna where the input power was 10 W and ablation time was 10 min. The SAR distribution to the liver tissue determines the lesion of the tumor cell and it directly depends on the antenna design and slot number.

Fig. 6 shows the variation of SAR with the insertion depth for monopole, single, and double slot antennae. The highest SAR distribution was found for the double slot antenna, which was 3500 W/kg at the insertion depth of the antenna 61 mm which was near the upper slot. For the single-slot antenna, the highest value for SAR is 3350 W/kg at the insertion depth of 63 mm near the slot, and the monopole antenna shows a SAR value of 2600 W/kg near the radiating segment. At the tip of the antenna, the SAR was 2490 W/kg and 2600 W/kg respectively for the double and single-slot antenna. For all cases, the highest SAR was found near the second slot of the double-slot antenna as shown in Table 3.

From the second slot the heat penetrated to the highest depth of the tissue. The result demonstrates that the highest temperature distribution and SAR are found within the insertion depth of 61 mm which is the upper slot of the double-slot antenna. Double slot antenna has a more organized thermal distribution pattern and tissue damage has the highest rate near the upper slot. The SAR distributions steadily rise along the Microwave antenna's longitudinal axis, peaking near the slot exit.

Table 5 summarizes the comparison of temperature distribution after the ablation time of 10 min at different insertion points for single-slot and double-slot antennae. In a double slot antenna, the temperature at a smaller penetration depth is higher than the single slot antenna. However, the temperature decreases much faster with the penetration depth than the single slot antenna. In addition, the fractional damage is also lower for the double-slot antenna. A double-slot antenna was developed to address the drawbacks of monopole and single-slot antennae. The earlier experiments like P. Keangin et al. [8], S. Kaur et al. [22] demonstrated that the dual-slot antenna outperforms the monopole and single-slot antenna in terms of high-power localization and peak SAR value was obtained near the slot similar to our study (see Table 6).

The backward heating was not eliminated in our current design. The

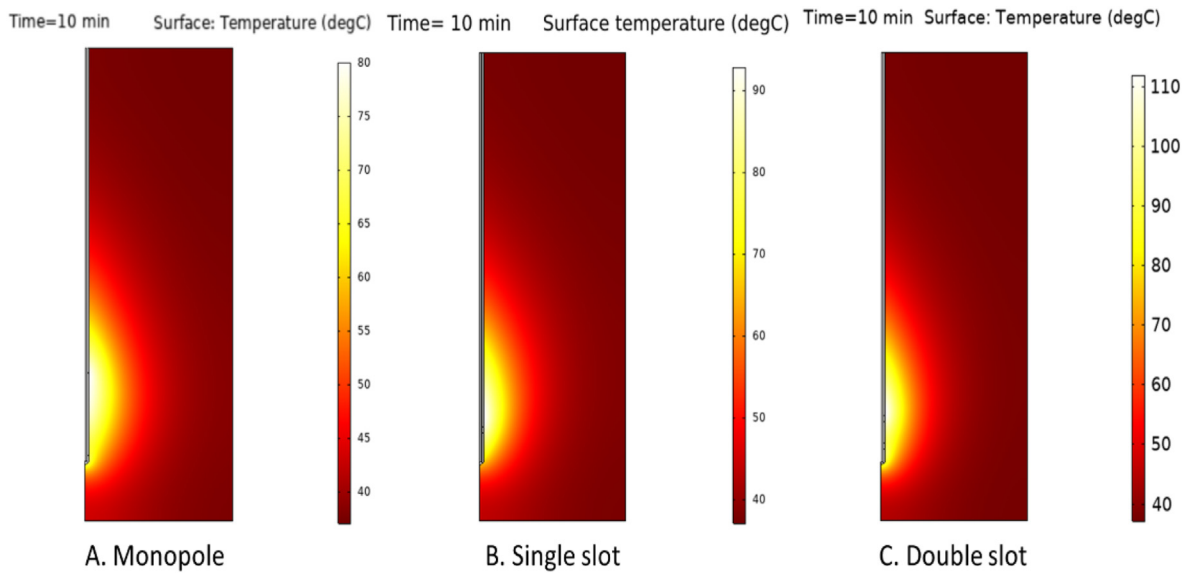

Fig. 4. The temperature profile for a 2D asymmetric view of an (a) monopole antenna, (b) single slot antenna, and (c) double slot antenna after 10 min ablation time.

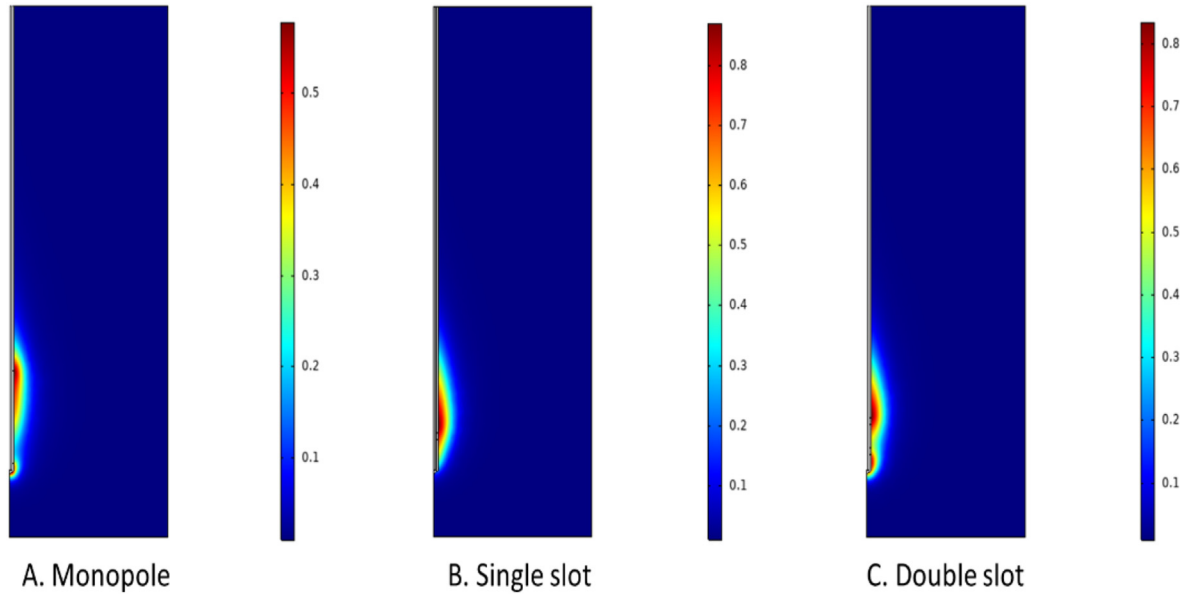

Fig. 5. The tissue damage rate for 0.5 min of thermal ablation for (a) monopole, (b) single slot antenna, and (c) double slot antenna.

Table 3
The comparison in the result of temperature distribution for different ablation times and different depth points, the fraction of damage, and SAR at different depths for single-slot and double-slot antennae.

Comparison Terms	Monopole	Single Slot	Double Slot
Temperature after 10 min	366 k	368 k	380 k
SAR at 2.5 mm	2600 W/kg	3350 W/kg	3500 W/kg
The temperature reaches 50 °C	2.1 min	1.86 min	1.2 min
Ablation diameter	2.0 cm	2.4 cm	3.5 cm
Ablation length	5.1 cm	6.5 cm	6.7 cm

purpose of our work was to present a systematic overview of the design procedure by considering the critical design parameters and to suggest ways to improve the performance of conventional slot antennae.

This study primarily focused on the design parameters of antenna slots and their outcomes concerning various ablation parameters. The objective is to identify antenna configurations that lead to a quicker attainment of an antenna temperature of 50 °C, alongside a viable ablation diameter for accelerated tumor cell destruction. To enhance the precision of this investigation, the study emphasizes SAR analysis and the fraction of damaged tissue, both contingent on a specific duration of power exposure. From the simulation results, we observed that the double-slot antenna exhibits more dissipation and greater SAR near the upper slot. The evolution of a lesion induced by the double-slot antenna displays a swifter and denser progression toward the upper slot, characterized by reduced insertion depth. Through a comprehensive analysis of simulation outcomes and parameter determinations, we conclude that the double-slot antenna holds greater promise in terms of feasibility, convenience, and efficiency for the treatment of tumor cells.

Indeed, as tumor shape and placement vary across different anatomical locations, it needs different antenna shapes and ablation

Table 4
SAR and thermal damage calculated at different depths and points. This result has been analyzed for near the tip and the slot and spherical heat distribution.

Slot position result analysis	Single Slot Antenna		Double Slot Antenna	
	Near slot	Near tip	Upper slot	Near tip
Temperature after 10min	368.68 K	347.56 K	380 K	361.03 K
Temperature reaches over 50 °C	0.30 min	1.86 min	0.23 min	1.2 min
Temperature after 0.25 min	325.62 K	321 K	330.37 K	323.81 K
SAR at 2.5 mm depth	3350 W/kg	2600 W/kg	3500 W/kg	2490 W/kg
SAR at 3.5 mm depth	1910 W/kg	1400 W/kg	2000 W/kg	1350 W/kg
Ablation diameter	2.4 cm	2.2 cm	3.5 cm	2.8 cm

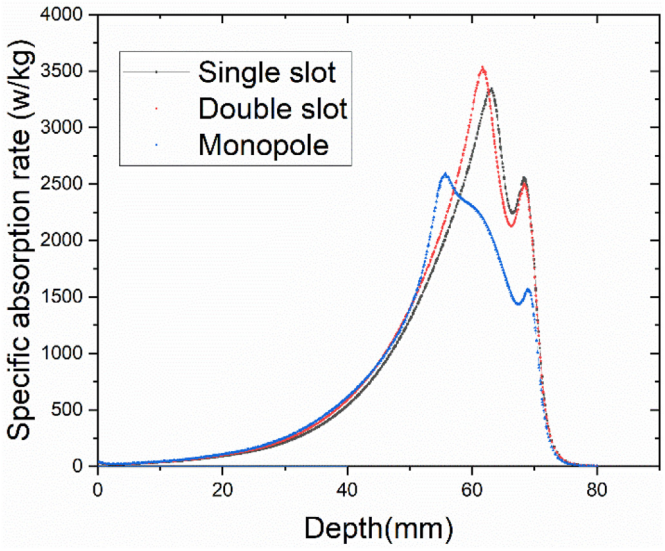

Fig. 6. The variation of SAR as a function of depth for three (monopole, single and double slot) designed antennae, which was calculated within 2.5 mm depth. A parallel line to the antenna has been taken for plotting a 2D line graph for SAR (W/kg) vs depth (mm).

ranges. Our current study has been focused on characterizing the double slot antenna specifically for liver tissue. Previously published literature demonstrates the effectiveness of microwave ablation, including slot antenna designs, in diverse tissue types such as bone and breast tissues [17,30]. A similar study can be performed by changing the tissue properties of this designed antenna. It is noted that this model does not consider the tumor shape and size for ablation therapy. The future work will be based on a 3D realistic model of liver tissue and tumor cells and demonstrate the effect of the antenna to examine the destructive area without damaging the surrounding healthy tissue.

4. Conclusion

This work evaluates the interstitial MWA and their characterization based on the antenna slot number and position. The result has been compared based on tissue damage fraction, thermal dissipation, and SAR. This study also determines the electromagnetic wave propagation connected to heat transport in the liver tissue utilizing a double and single-slot antenna to find out the best applicator for a certain treatment region. Extensive investigations showed that the SAR and thermal distribution depend on the size, design, and location of the slot. The study reveals that the highest temperature and SAR reading are found near the upper slot of the double slot antenna for all the cases. The heat penetrated more depth into liver tissue for single slot antenna which has a higher possibility to damage surrounding healthy tissue. However, for double-slot antennae, the formation of tissue damage has the highest rate and is faster and denser at the location near the upper slot and has the higher ablation area. Although the current model is only applicable to liver tissue ablation, however, this model could be effectively extended to other organ tumor ablation processes incorporating relevant parameters of other organs. This information would be helpful for a basic understanding of the MWA process in different tissues and for finding out the critical design parameters for enhancing performance.

Table 6
Comparison of SAR and Temperature value of our present study with previously published work.

Result Analysis	Present Experiment	P. Keangin et al. [8]	S. Kaur et al. [22]
Highest SAR	3.1 kW/kg	2.7 kW/kg	3.04 kW/kg
Highest Temperature	107 °C	85.5 °C	101 °C

Author contributions

Sabiha Binte Aziz and Torikul Islam: Methodology, Software, Investigation, Writing- Original draft preparation. Md Rejvi Kaysir and Md Jahirul Islam: Conceptualization, Visualization, Data curation, Supervision, Writing- Reviewing and Editing. Mahmadur Rahman: Writing-Reviewing and Editing.

Table 5
The comparison of the *temperature distribution* after 10 min of ablation time and *fraction of damage* at different depth points for both single-slot and double-slot antennae.

Depth point temperature analysis for slot antenna	5 mm depth (5,20) point	10 mm depth (10,20) point	15 mm depth (15,20) point	20 mm depth (20,20) point	25 mm depth (25,20) point
Temperature after 10 min (single slot)	345 K	326 K	317.5 K	315.5 K	312 K
Temperature after 10 min (Double slot)	357 K	326 K	318 K	313 K	311 K
Fraction of damage at (single slot)	~3.5 min	~8 min	No tissue damage	No tissue damage	No tissue damage
Fraction of damage at (Double slot)	~2.2 min	~6.5 min	No tissue damage	No tissue damage	No tissue damage

Funding

None.

Ethical approval

Not required.

Declaration of competing interest

The authors declare that they have no known competing financial interests or personal relationships that could have appeared to influence the work reported in this paper.

Acknowledgements

This study was supported by the facilities provided by Khulna University of Engineering & Technology (KUET), Bangladesh.

References

[1] Lubner MG, Brace CL, Ziemlewicz TJ, Hinshaw JL, Lee FT. Microwave ablation of hepatic malignancy. Semin Intervent Radiol 2013;30:56–66. https://doi.org/10.1055/s-0033-1333654.
[2] Chang IA. Considerations for thermal injury analysis for RF ablation devices. Open Biomed Eng J 2010;4:3–12. https://doi.org/10.2174/1874120701004020003.
[3] Prakash P. Theoretical modeling for hepatic microwave ablation. Open Biomed Eng J 2010;4:27–38. https://doi.org/10.2174/1874120701004020027.
[4] Brace C. Thermal tumor ablation in clinical use. IEEE Pulse 2011;2:28–38. https://doi.org/10.1109/MPUL.2011.942603.
[5] Brace CL, Hinshaw JL, Laeseke PF, Sampson LA, Lee FT. Pulmonary thermal ablation: comparison of radiofrequency and microwave devices by using gross pathologic and CT findings in a swine model. Radiology 2009;251:705–11. https://doi.org/10.1148/radiol.2513081564.
[6] Tehrani MHH, Soltaniid M, Soltaniid M, Soltaniid M, Soltaniid M, Soltaniid M, et al. Use of microwave ablation for thermal treatment of solid tumors with different shapes and sizes-A computational approach. PLoS One 2020;15:e0233219. https://doi.org/10.1371/journal.pone.0233219.
[7] Collins Jarrod A, Heiselman Jon S, Clements Logan W, Daniel B, Brown MIM. Multiphysics modeling toward enhanced guidance in hepatic microwave ablation: a preliminary framework. J Med Imaging 2019;6:025007. https://doi.org/10.1117/1.jmi.6.2.025007.
[8] Keangin P, Rattanadecho P, Wessapan T. An analysis of heat transfer in liver tissue during microwave ablation using single and double slot antenna. Int Commun Heat Mass Tran 2011;38:757–66. https://doi.org/10.1016/j.icheatmasstransfer.2011.03.027.
[9] Lee M, Son T. Helical slot antenna for the microwave ablation. Int J Antenn Propag 2019;2019:2126879. https://doi.org/10.1155/2019/2126879.
[10] Brace CL, Laeseke PF, Van Der Weide DW, Lee FT. Microwave ablation with a triaxial antenna: results in ex vivo bovine liver. IEEE Trans Microw Theor Tech 2005;53:215–20. https://doi.org/10.1109/TMTT.2004.839308.
[11] Prakash P, Converse MC, Webster JG, Mahvi DM. An optimal sliding choke antenna for hepatic microwave ablation. IEEE Trans Biomed Eng 2009;56:2470–6. https://doi.org/10.1109/TBME.2009.2025264.
[12] Fallahi H, Prakash P. Antenna designs for microwave tissue ablation. Crit Rev Biomed Eng 2018;46:495–521. https://doi.org/10.1615/CritRevBiomedEng.2018028554.
[13] Ibitoye AZ, Orotoye T, Nwoye EO, Aweda MA. Analysis of efficiency of different antennas for microwave ablation using simulation and experimental methods. Egypt J Basic Appl Sci 2018;5:24–30. https://doi.org/10.1016/j.ejbas.2018.01.005.
[14] Adewumi O, Agbasi O, Fatile O. Effect of water-cooled loop monopole antenna on microwave ablation efficiency. Mehmet Akif Ersoy Üniversitesi Sağlık Bilim Enstitüsü Derg 2019;7:41–54. https://doi.org/10.24998/maeusabed.590456.
[15] Ibitoye ZA, Nwoye EO, Aweda MA, Oremosu AA, Annunobi CC, Akanmu ON. Optimization of dual slot antenna using floating metallic sleeve for microwave ablation. Med Eng Phys 2015;37:384–91. https://doi.org/10.1016/j.medengphy.2015.01.015.
[16] Maltzahn G Von, Park JH, Agrawal A, Bandaru NK, Das SK, Sailor MJ, et al. Computationally guided photothermal tumor therapy using long-circulating gold nanorod antennas. Cancer Res 2009;69:3892–900. https://doi.org/10.1158/0008-5472.CAN-08-4242.
[17] Trujillo-Romero CJ, Leija-Salas L, Vera-Hernández A, Rico-Martínez G, Gutiérrez-Martínez J. Double slot antenna for microwave thermal ablation to treat bone tumors: modeling and experimental evaluation. Electron 2021;10:761. https://doi.org/10.3390/electronics10070761.
[18] Sawicki JF, Shea JD, Behdad N, Hagness SC. The impact of frequency on the performance of microwave ablation. Int J Hyperther 2017;33:61–8. https://doi.org/10.1080/02656736.2016.1207254.
[19] Yue W, Wang S, Yu S, Wang B. Ultrasound-guided percutaneous microwave ablation of solitary T1N0M0 papillary thyroid microcarcinoma: initial experience. Int J Hyperther 2014;30:150–7. https://doi.org/10.3109/02656736.2014.885590.
[20] Wang T, Zhao G, Qiu B. Theoretical evaluation of the treatment effectiveness of a novel coaxial multi-slot antenna for conformal microwave ablation of tumors. Int J Heat Mass Tran 2015;90:81–91. https://doi.org/10.1016/j.ijheatmasstransfer.2015.06.030.
[21] Simo KA, Tsirline VB, Sindram D, McMillan MT, Thompson KJ, Swan RZ, et al. Microwave ablation using 915-MHz and 2.45-GHz systems: what are the differences? HPB 2013;15:991–6. https://doi.org/10.1111/hpb.12081.
[22] Kaur S, Mann PS. Comparison of single slot and double slot antenna for the treatment of hepatocellular carcinoma. Int J Res Comput Appl Robot 2014;2:86–91.
[23] Jesús MF, Rubio C, Hernández AV, Salas LL, Ávila-Navarro E, Navarro EA. Coaxial slot antenna design for microwave hyperthermia using finite-difference time-domain and finite element method. Open Nanomed J 2011;3:2–9. https://doi.org/10.2174/1875933501103010002.
[24] Schaible J, Lürken L, Wiggermann P, Verloh N, Einspieler I, Zeman F, et al. Primary efficacy of percutaneous microwave ablation of malignant liver tumors: comparison of stereotactic and conventional manual guidance. Sci Rep 2020;10:18835. https://doi.org/10.1038/s41598-020-75925-6.
[25] Ge M, Jiang H, Huang X, Zhou Y, Zhi D, Zhao G, et al. A multi-slot coaxial microwave antenna for liver tumor ablation. Phys Med Biol 2018;63:175011. https://doi.org/10.1088/1361-6560/aad9c5.
[26] Tucci C, Trujillo M, Berjano E, Iasiello M, Andreozzi A, Vanoli GP. Pennes' bioheat equation vs. porous media approach in computer modeling of radiofrequency tumor ablation. Sci Rep 2021;11:5272. https://doi.org/10.1038/s41598-021-84546-6.
[27] Yang D, Converse MC, Mahvi DM, Webster JG. Measurement and analysis of tissue temperature during microwave liver ablation. IEEE Trans Biomed Eng 2007;54:150–5. https://doi.org/10.1109/TBME.2006.884647.
[28] Palash TI, Kaysir MR, Islam MJ, Aziz SB, Mimma TN, Akther N. In-silico performance investigation of nanoparticle-assisted photo thermal ablation. J Biol Syst 2023;31:93–113. https://doi.org/10.1142/S0218339023500055.
[29] Yang D, Converse MC, Mahvi DM, Webster JG. Expanding the bioheat equation to include tissue internal water evaporation during heating. IEEE Trans Biomed Eng 2007;54:1382–8. https://doi.org/10.1109/TBME.2007.890740.
[30] Ortega-Palacios R, Trujillo-Romero CJ, Rubio MFJC, Vera A, Leija L, Reyes JL, et al. Feasibility of using a novel 2.45 GHz double short distance slot coaxial antenna for minimally invasive cancer breast microwave ablation therapy: computational model, phantom, and in vivo swine experimentation. J Healthc Eng 2018;2018:5806753. https://doi.org/10.1155/2018/5806753.